Relationship Between the Physicochemical Properties of Lipid Nanoparticles and the Quality of siRNA Delivery to Liver Cells

Yusuke Sato[1], Hiroto Hatakeyama[1], Mamoru Hyodo[1] and Hideyoshi Harashima[1]

[1]*Laboratory for Molecular Design of Pharmaceutics, Faculty of Pharmaceutical Sciences, Hokkaido University, Kita-12, Nishi-6, Kita-Ku, Sapporo 060-0812, Japan*

While a variety of short interfering RNA (siRNA) delivery compounds have been developed, a deep understanding of the key parameters that determine the quality of siRNA delivery are not known with certainty. Therefore, an understanding of the factors required for the efficient, selective, and safe delivery of siRNA is a great challenge for successful siRNA delivery. Herein, we report on the development of two pH-sensitive cationic lipids and their use in examining the impact of the acid dissociation constant (pK_a) value, lipase sensitivity and the size of lipid nanoparticles on the biodistribution, and efficiency and cell specificity of gene silencing in the liver. An increase in the pK_a value resulted in a significant change in the intrahepatic localization of siRNA and gene-silencing efficiency in hepatocytes and liver sinusoidal endothelial cells (LSECs). The sensitivity of the pH-sensitive cationic lipid to lipases was a major factor in achieving hepatocyte-specific gene silencing. Increasing the particle size can improve the LSEC specificity of gene silencing. As a consequence, we succeeded in developing both a highly efficient, hepatocyte-specific formulation, and the most efficacious LSEC-targeted formulation reported to date. These findings will facilitate the development of more sophisticated siRNA delivery systems.

Received 26 May 2015; accepted 1 October 2015; advance online publication 26 January 2016. doi:10.1038/mt.2015.222

INTRODUCTION

Since the discovery of RNA interference (RNAi),[1] short interfering RNA (siRNA)-mediated RNAi medicine has been predicted to be a valuable approach to treating various diseases. To induce RNAi-mediated gene silencing, the siRNA must reach the cytosol where it forms an active complex with an RNAi-induced silencing complex in target cells. However, owing to the physicochemical properties of siRNA, which include a relatively high molecular weight, an anionic charge, and hydrophilicity, it is unable to pass through biomembranes to reach target cells. Therefore, delivery vehicles are required to improve the pharmacological properties of siRNA.[2] However, doing this effectively and selectively remains a major obstacle. A variety of siRNA delivery materials have been developed to date.[3,4] However, detailed information regarding the key factors that determine the quality of siRNA delivery are still lacking and it is essential that these factor be clarified, if sophisticated siRNA carriers for *in vivo* gene analysis and clinical applications are to be realized.

Since hepatocytes are involved in a variety of liver diseases including metabolic disorders, hepatitis, and cancer, most research has focused on the same cell type. However, liver tissue consists of several cell types including hepatocytes, liver sinusoidal endothelial cells (LSECs), and Kupffer cells. The important functions of the LSECs on the immune response,[5] lipid metabolism,[6] and metastasis[7] are currently in the process of being elucidated. Therefore, technology for the specific and efficient delivery of siRNA to hepatocytes and LSECs is necessary to analyze their functions *in vivo* directly.

To address this problem, we developed and used a multifunctional envelope-type nanodevice (MEND), which was previously developed for use as a nucleic acid carrier.[8] We previously synthesized a pH-sensitive cationic lipid, YSK05,[9] and succeeded in delivering nucleic acids to liver,[10] tumor tissue,[11] and the brain[12] and treating hepatitis C virus infections in chimeric mice with humanized livers.[13] We recently synthesized a pH-sensitive cationic lipid YSK13-C3 and a MEND containing the YSK13-C3 (YSK13-C3-MEND) achieved a median effective dose (ED_{50}) of 0.015 mg/kg on coagulation factor VII (FVII) silencing in healthy mice and the treatment of a hepatitis B virus infection.[14] Herein, we report on the development of a series of two pH-sensitive cationic lipids (referred as YSK13 and YSK15) with different pK_a values (**Figure 1**). First, we characterized the physical properties of the pH-sensitive cationic lipids and their MENDs. Furthermore, the impact of the key parameters including pK_a value, lipase sensitivity and the size of the lipid nanoparticles (LNPs) on biodistribution, and the efficiency and cell specificity of gene silencing in liver cells were elucidated separately.

RESULTS

Characterization of pH-sensitive cationic lipids and MENDs

The synthetic procedure and chemical characterization of the YSK13 and YSK15 are shown in the **Supplementary Materials**

Correspondence: Hideyoshi Harashima, Faculty of Pharmaceutical Science, Hokkaido University, Sapporo, Hokkaido, 060-0812, Japan.
E-mail: harasima@pharm.hokudai.ac.jp

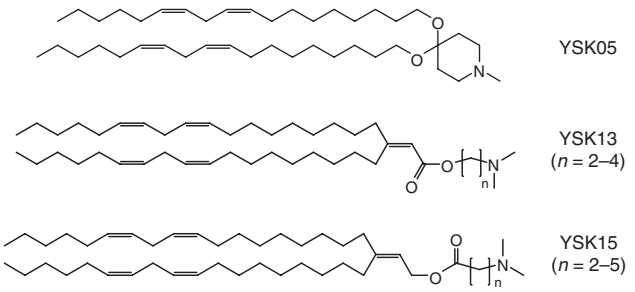

Figure 1 Structures of the pH-sensitive cationic lipids used in this study.

and Methods. The YSK13 and YSK15 preparations include three and four kinds of lipid structures that contain different numbers of methylene units between a dimethylamino moiety and an ester bond (**Figure 1**). These lipids are distinguished based on the number of methylene units they contain. For example, the YSK13 containing two methylene units is denoted as YSK13-C2. In this study, YSK05 was utilized as a control lipid (**Figure 1**).

The membrane disruption activity of YSK13 was evaluated by ^{31}P nuclear magnetic resonance (NMR) analysis using a lipid dispersion composed of equimolar amounts of a pH-sensitive cationic lipid, 1-palmitoyl-2-oleoyl-*sn*-glycero-3-phosphatidylcholine (POPC), and 1,2-distearoyl-*sn*-glycero-3-phosphatidylserine (DSPS) suspended in an acidic buffer at pH 4.0. It is known that a lamellar and an inverted hexagonal (H_{II}) phase show a broad signal with a high-field peak and a low-field peak, respectively.[15] In this assay, a higher transition temperature required to convert a lamellar phase into an H_{II} phase (T_H) indicated a decreased membrane disruption activity. For YSK05, a lamellar phase was observed at 21 °C and the H_{II} phase-derived peak first appeared at 25 °C (arrow), indicating that the T_H value of YSK05 was between 21 and 25 °C under these experimental conditions (**Figure 2a–c**). All three types of YSK13 preparations showed a clear H_{II} phase at 21 °C (**Figure 2d–f**), indicative of their having a higher membrane disruption activity than YSK05. This result corresponds to a previous finding showing that the YSK13-C3-MEND showed a higher gene-silencing activity in hepatocytes (ED_{50}: 0.015 mg/kg) than the YSK05-MEND (ED_{50}: 0.06 mg/kg).[13]

MENDs were prepared by the *tert*-butanol injection procedure[9] with the following lipid composition: pH-sensitive cationic lipid, cholesterol, and 1,2-dimirystoyl-*sn*-glycero methoxyethyleneglycol 2000 ether (PEG-DMG) at a molar ratio of 70/30/3, respectively. All of the MENDs had a similar size (~75 nm) with a low polydispersity index (~0.1), a near-neutral ζ-potential (−5 to +10 mV) at pH 7.4 and a high siRNA encapsulation efficiency (90–95%) (**Supplementary Table S1**). The pK_a value of the MENDs was measured by the fluorescent intensity of 2-(*p*-toluidino)-6-naphthalenesulfonic acid (TNS). TNS fluoresces only when it is associated with a positively charged membrane and is utilized to detect them.[16,17] A TNS fluorescent assay revealed that the YSK13 and the YSK15 had various apparent pK_a values ranging from 5.70 to 6.80 and 5.80 to 7.25, respectively, depending on the number of methylene units contained. The percentages of cationically charged lipid at pH 7.4 were calculated using the Henderson–Hasselbalch equation and the results are shown in **Supplementary Table S1**.

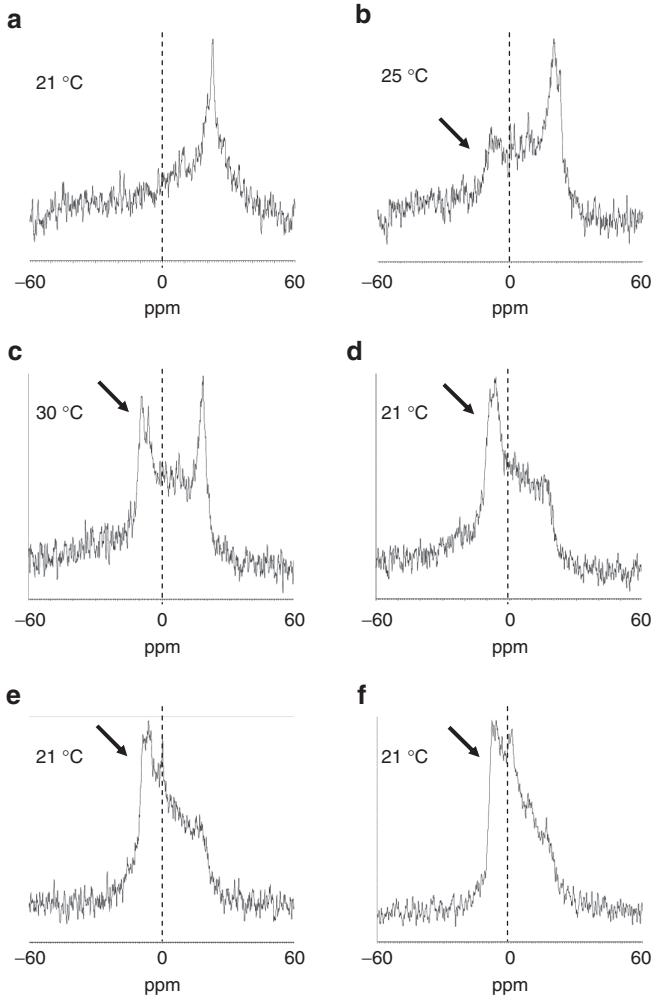

Figure 2 Measurement of the phase transition temperature by ^{31}P NMR. The pH-sensitive cationic lipid was incorporated into a lipid dispersion with the neutral lipid POPC and the negatively charged lipid DSPS at a molar ratio of 1:1:1. Arrows indicate the signal of an inverted hexagonal phase. (**a–c**) YSK05. (**d**) YSK13-C2. (**e**) YSK13-C3. (**f**) YSK13-C4. DSPS, 1,2-distearoyl-*sn*-glycero-3-phosphatidylserine; NMR, nuclear magnetic resonance; POPC, 1-palmitoyl-2-oleoyl-*sn*-glycero-3-phosphatidylcholine.

Impact of pK_a value on cell specificity

The gene-silencing activity of these MENDs in two major hepatic cells including hepatocytes and LSECs, which play an important role in immune response and tumor metastasis,[5,7] was examined. The target genes of the siRNAs for hepatocytes and LSECs were FVII and CD31, respectively. In hepatocytes, a plot of ED_{50} for gene silencing versus the pK_a value indicated a bell-shaped curve with a maximal activity at a pK_a of 6.45 (**Figure 3a**). This result is in agreement with previously reported findings.[18] On the other hand, in LSECs, a plot of CD31 expression versus pK_a value indicated a sigmoid curve with an increase in gene-silencing efficiency in response to a rise of pK_a value (**Figure 3b**), which was quite different from that in hepatocytes. Based on this result, it was revealed that the pK_a value clearly determines, not only gene-silencing

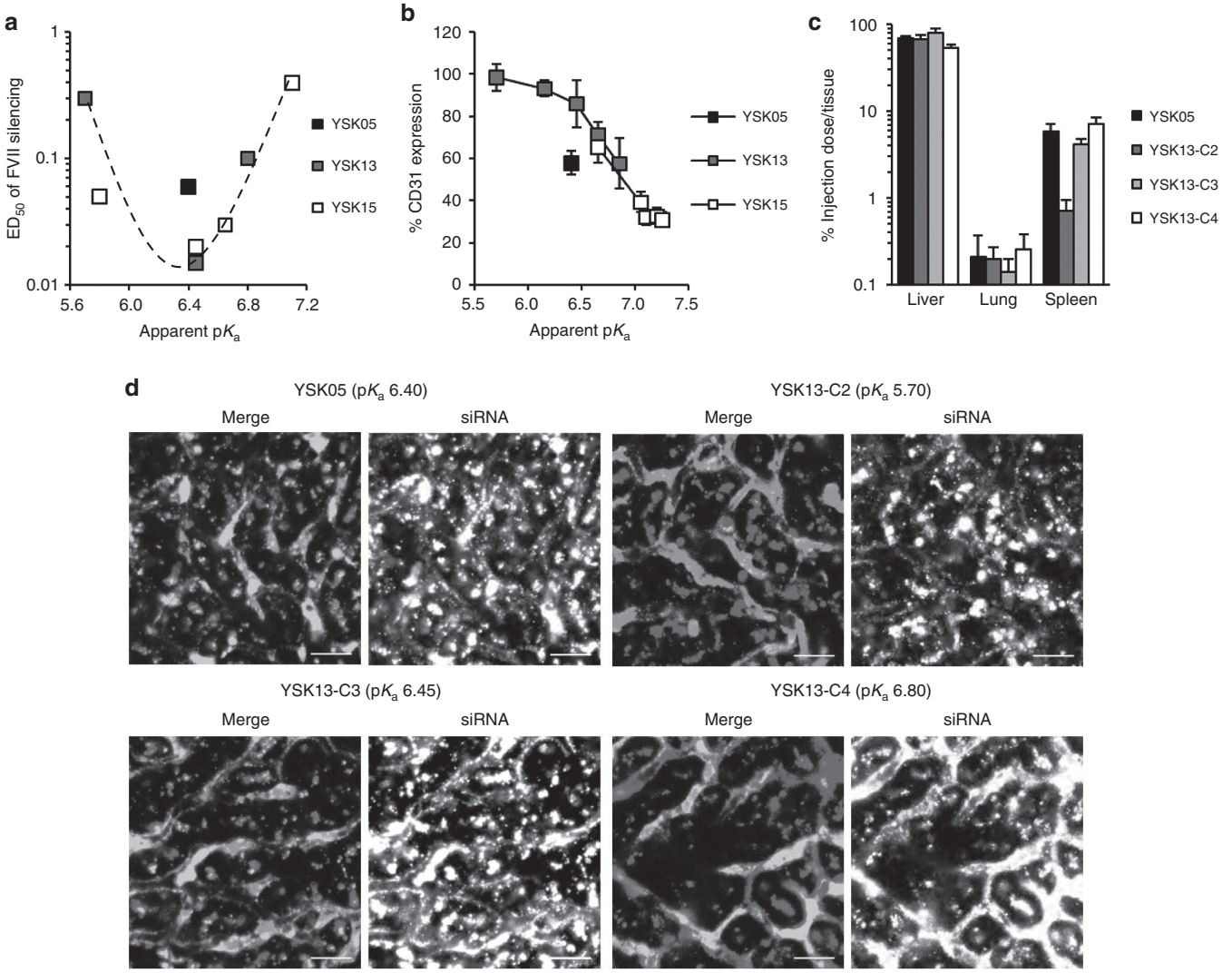

Figure 3 pK_a dependency of *in vivo* gene-silencing activity and siRNA biodistribution. (**a**) A plot of the ED_{50} for FVII gene silencing versus pK_a value of MENDs. Mice were i.v. injected with siFVII encapsulated in MENDs composed of each pH-sensitive cationic lipid, plasma FVII activity was measured, and ED_{50} was determined from a dose–response curve. (**b**) A plot of CD31 expression in liver and pK_a value of MENDs. Mice were i.v. injected with siCD31 encapsulated in MENDs composed of each pH-sensitive cationic lipid, and CD31 mRNA expression in liver was determined by quantitative reverse transcription–PCR. (**c**) Systemic distribution of siRNAs formulated in YSK05-MEND and three kinds of YSK13-MENDs. Mice were i.v. injected with MENDs encapsulating Cy5-labeled siRNAs at 0.5 mg/kg. Tissues were collected, homogenized, and the fluorescent intensity of Cy5 was measured in 30 minutes. Data are represented as the mean ± SD (n = 3). (**d**) Intrahepatic distribution of siRNAs formulated in YSK05-MEND and three kinds of YSK13-MENDs. Mice were i.v. injected with MENDs encapsulating Cy5-labeled siRNAs at 1 mg/kg. Liver tissues were collected, and blood vessels were stained with FITC-conjugated Isolectin B4. Blood vessels and siRNAs are visualized as green and red, respectively. Bars represent 20 µm. ED_{50}, median effective dose; FVII, factor VII; MEND, multifunctional envelope-type nanodevice.

activity in hepatocytes, but in LSECs as well. To investigate the impact of the pK_a value on biodistribution, we measured the accumulation of siRNA in some tissues. The results showed that liver accumulation was substantially higher than that for the lung and spleen and was similar in the range of 5.70–6.80 (**Figure 3c**). Splenic accumulation increased in response to an increase in the pK_a value. We next observed the intrahepatic distribution of siRNA and found a dramatic change from the extravascular region where hepatocytes exist to blood vessels in response to the rise in the pK_a value in the range of 5.70–6.80 (**Figure 3d**). On the other hand, in the pK_a range of 6.65–7.25, siRNA localization in blood vessels clearly decreased in response to an increase in the pK_a value (**Supplementary Figure S1**).

It has been reported that apolipoprotein E (ApoE) binds to liposomes and acts as an endogenous ligand for hepatocytes.[19,20] Therefore, we examined the involvement of the ApoE on the uptake of siRNA by LSECs in ApoE-deficient mice and the results indicated that gene-silencing activity on LSECs was significantly enhanced by coinjection of the recombinant human ApoE3 protein, while the impact of the ApoE on LSECs was lower compared to that on hepatocytes (**Supplementary Figure S2**). Among the several MENDs used in this study, the YSK15-C4-MEND (pK_a 7.10) conferred the strongest gene-silencing activity in LSECs (ED_{50}: 0.1 mg/kg) but no gene silencing in other organs was found at a dose of 0.3 mg/kg (**Supplementary Figure S3**).

Impact of lipase sensitivity on cell specificity

Whereas the YSK05-MEND and the YSK13-C3-MEND had similar pK_a values for liver accumulation and intrahepatic distribution (**Supplementary Table S1** and **Figure 3c,d**), we found that the hepatocyte specificity of the YSK13-C3-MEND on gene silencing was much higher than that for the YSK05-MEND (>67-fold and 8.3-fold, respectively) (**Figure 4a**). It is known that there are three types of extracellular lipases including hepatic lipase (HL), endothelial lipase (EL), and lipoprotein lipase (LPL) on the surface of cell membranes in liver tissue.[21] HL is present only on the surface of hepatocytes, whereas the EL and LPL are present on the surface of LSECs.[22,23] Based on this knowledge, we hypothesized that the YSK13, which has an ester bond as a linker, was degraded and inactivated by the activity of either EL or LPL on the surface of LSECs but not on the surface of hepatocytes and in the blood circulation. To reveal the involvement of the EL or LPL on hepatocyte specificity, the CD31 gene-silencing activity of the YSK13-C3-MEND in liver was measured with or without a cotreatment with GSK264220A (an inhibitor of both EL and LPL)[24] and orlistat (an inhibitor of LPL).[25] The activity of the YSK13-C3-MEND was enhanced only in the case of the cotreatment of the GSK264220A (**Figure 4b**), suggesting that the YSK13-C3-MEND is inactivated by the activity of EL. Moreover, we evaluated the effect of the cotreatment of the GSK264220A on FVII gene-silencing activity. The siFVII dose was set at 0.1 mg/kg and 0.01 mg/kg on the YSK05-MEND and YSK13-C3-MEND, respectively. No significant change of the gene-silencing efficiency of both formulations was observed by cotreatment of the GSK264220A (**Supplementary Figure S4**).

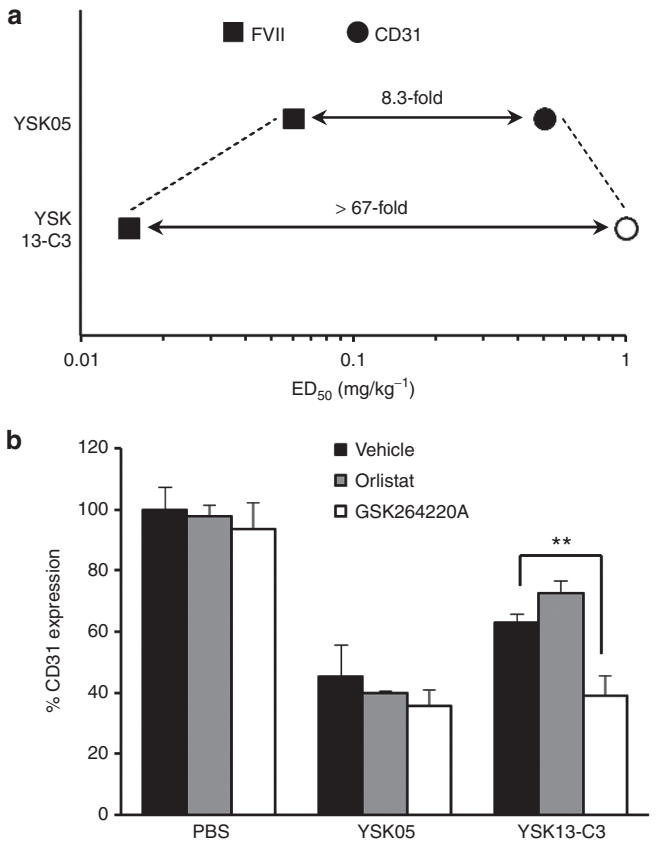

Figure 4 High hepatocyte specificity of YSK13-C3-MEND by sensitivity toward activity of lipase. (**a**) A plot of ED_{50} for *in vivo* gene silencing of YSK05-MEND and YSK13-C3-MEND in hepatocytes and LSECs. For YSK13-C3-MEND, ED_{50} dose was not achieved in LSECs, this is indicated by the open circle representing the highest dose tested. (**b**) Effect of lipase inhibitors on CD31 gene-silencing activity in liver. Mice were i.p. injected with GSK264220A (30 mg/kg), orlistat (30 mg/kg), or vehicle and i.v. injected with siCD31 formulated in the YSK05-MEND or the YSK13-C3-MEND at a dose of 1 mg/kg. CD31 mRNA expression in liver tissue was quantified in 24 hours. Data are represented as the mean ± SD (n = 3). **P < 0.01 (by two-tail unpaired t-test). ED_{50}, median effective dose; FVII, factor VII; LSEC, liver sinusoidal endothelial cell; MEND, multifunctional envelope-type nanodevice; PBS, phosphate-buffered saline.

Impact of size on cell specificity

The impact of particle size on gene-silencing activity in hepatocytes and LSECs was investigated next. For hepatocytes, the YSK13-C3-MEND, the pK_a value of which is optimal for gene silencing in hepatocytes, was used. As shown in **Figure 5a**, the 76.5- and 117-nm-sized MENDs showed similar and high gene-silencing activity. On the other hand, a size-dependent and significant reduction in gene silencing was observed in the case of 172- and 433-nm-diameter particles. For LSECs, the

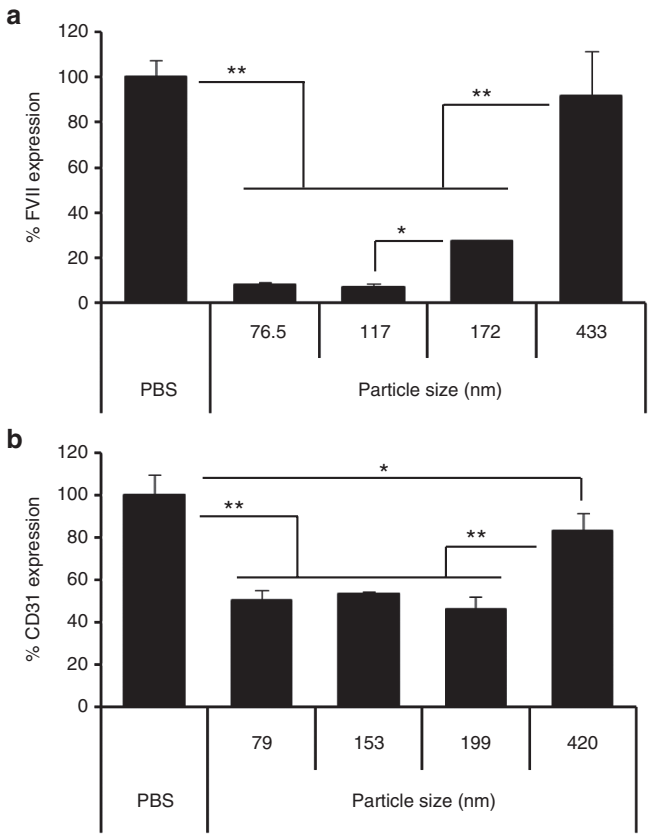

Figure 5 Impact of size on gene silencing in hepatocytes and in LSECs. (**a**) Mice were injected with siFVII formulated in YSK13-C3-MENDs with various size at 0.1 mg/kg and plasma FVII activities were measured in 24 hours. (**b**) Mice were injected with siCD31 formulated in YSK15-C4-MENDs with various size at 0.1 mg/kg and CD31 mRNA expression on LSECs were quantified in 24 hours. Data are represented as the mean ± SD (n = 3). *P < 0.05, **P < 0.01 (by one-way nrANOVA, followed by SNK test). ANOVA, analysis of variance; FVII, factor VII; LSEC, liver sinusoidal endothelial cell; MEND, multifunctional envelope-type nanodevice; nrANOVA, non-repeated analysis of variance; PBS, phosphate-buffered saline; SNK, Student-Newman-Keuls.

YSK15-C4-MEND, which has an optimal pK_a for gene silencing in LSECs, was used. As shown in **Figure 5b**, similar gene-silencing activity was observed between 79 and 199 nm. The size range for efficient gene silencing in LSECs (79–199 nm) was wider than that in hepatocytes (76.5–117 nm). Therefore, it can be concluded that adjusting the particle size to ~200 nm leads to an increase in LSEC specificity.

Toxicity

Finally, the toxicity of the YSK13-C3-MEND was evaluated and no increase in aspartate aminotransferase or alanine aminotransferase and no loss in body weight was found at a dose of 0.3–1 mg/kg (**Figure 6**). This result shows that the YSK13-C3-MEND was well tolerated at a dose up to 100-fold higher than FVII ED_{50}.

DISCUSSION

In this study, a series of two pH-sensitive cationic lipids, referred as YSK13 and YSK15, were synthesized (**Figure 1**). These lipids were designed based on the following three strategies. First, two long unsaturated acyl chains were incorporated to emphasize the bulkiness of the hydrophobic region to enhance membrane destabilization activity.[26] For the same reason, a carbon–carbon double bond between two acyl chains was also incorporated; notably, the bond angle of an sp^2 carbon was fixed at 120°, which is larger than that of an sp^3 carbon (~109.5°). This strategy contributed to the enhancement in fusogenic activity (**Figure 2**) and gene-silencing activity in hepatocytes (**Figure 3a**). Second, an ester bond was incorporated as a linker in order to produce a compound that can be degraded by innate lipases. Third, both the YSK13 and YSK15 series were designed to examine the effect of the direction of the ester bond on siRNA delivery.

In **Figure 3d**, the three kinds of YSK13-MENDs showed a quite different intrahepatic distribution, suggesting that a small difference in the pK_a value dramatically affects the intrahepatic distribution of siRNA, which reflects gene-silencing activity in both hepatocytes and LSECs (**Figure 3a**,**b**) The YSK13-C4-MEND (pK_a 6.80) and YSK15-C3-MEND (pK_a 6.65) showed the highest localization to LSEC in each lipid series (**Figure 3d** and **Supplementary Figure S1**), indicating that a slight cationic property (pK_a of 6.65–6.80, corresponding to a 15–20% cationic charge at pH 7.4) is suitable for the localization of siRNA to LSECs. Additionally, both the YSK05-MEND and YSK13-C3-MEND, which have a pK_a of 6.40–6.45 (only 9.1–10.1% of the pH-sensitive cationic lipids are cationic form), were partially taken up by LSECs (**Figure 3d**). This result indicates that a pK_a of ~6.4 is not optimal value in the light of hepatocyte-specific gene silencing, whereas the same pK_a value is optimal for gene-silencing activity in hepatocytes as shown in **Figure 3a** and in a previous report.[18] As the YSK13-C2-MEND (pK_a 5.70) was specifically taken up by hepatocytes (**Figure 3d**), a lower pK_a value would be expected to result in hepatocyte-specific gene silencing. However, the gene-silencing activity in hepatocytes dramatically decreases in response to a decline in the pK_a value, as shown in **Figure 3a**, because the formulation with low pK_a cannot convert to a cationic property in endosome, which results in poor endosomal escape. Therefore, a different mechanism except the pK_a value should be introduced to strike a balance between specificity and activity in hepatocytes.

As shown in **Supplementary Table S1**, the ζ-potentials of the MENDs at pH 7.4 were near-neutral indicating a low correlation with intrahepatic distribution (*i.e.*, uptake efficiency to LSECs). There are two possible reasons for this. First, a 100% siRNA encapsulation was not achieved (*i.e.*, about 4–10% of the siRNAs are not encapsulated). The surface of the MEND containing pH-sensitive cationic lipids must be cationic, although the degree of the cationic intensity depends on their apparent pK_a value. Therefore, the negatively charged siRNAs which are present outside of the MENDs would be expected to interact with the surface of the MENDs. As a result, the ζ-potential of the MENDs tends to be neutral (sometimes slightly negative). Moreover, the siRNAs that become attached to the surface of the MENDs can be rapidly released in the blood stream. Second, the MENDs are covered with 3 mol% of PEG-DMG, which partially shields the ζ-potential of the MENDs by forming a thick hydrated layer.[27] However, the PEG-DMG, which has two short hydrocarbon chains (C14), is known to be rapidly released from LNPs in the blood circulation.[28] Taken together, the ζ-potential of the MENDs in buffer are poor indicators of the actual charge state in an *in vivo* situation. On the other hand, a fluorescent probe, TNS, interacts directly with the positively charged pH-sensitive cationic lipids directly. Therefore, the apparent pK_a value of the pH-sensitive cationic lipid, which

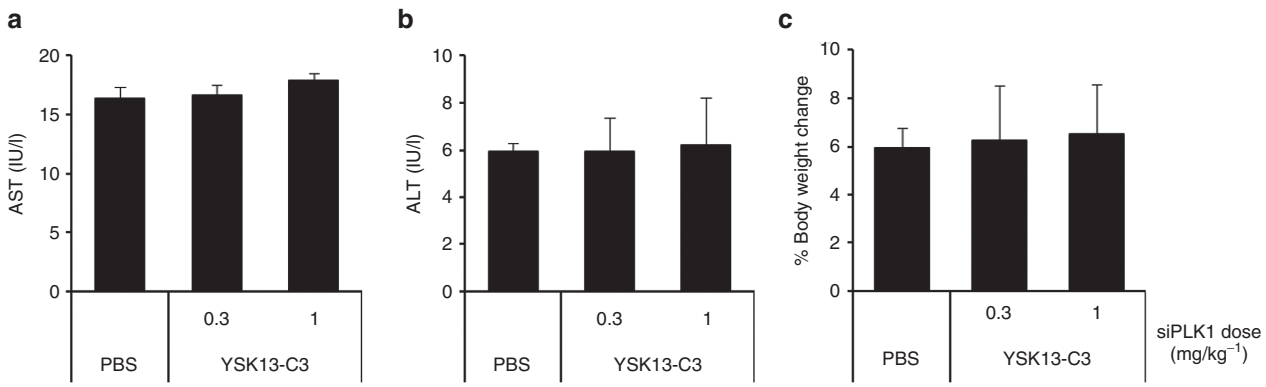

Figure 6 Hepatic and systemic toxicity of YSK13-C3-MEND. Mice were injected with siPLK1 formulated in YSK13-C3-MEND at 0.3 and 1 mg/kg. (**a**) AST and (**b**) ALT levels in plasma were measured. (**c**) Body weight was measured just before injection and at 24 hours. Data are expressed as a percentage of weight change. Data are represented as the mean ± SD (n = 3). ALT, alanine aminotransferase; AST, aspartate aminotransferase; MEND, multifunctional envelope-type nanodevice; PBS, phosphate-buffered saline; PLK1, polo-like kinase 1.

can be determined by a TNS assay, reflects the real charge state of the MEND surface and is correlated with the uptake efficiency to LSECs.

Although coinjection of ApoE with the YSK13-C3-MEND resulted in increase of gene-silencing efficiency in ApoE-deficient mice, the impact in LSEC was lower than that in hepatocytes (**Supplementary Figure S2**). As shown in **Figure 3d**, the YSK13-C2-MEND, which has only a 2% cationic charge in the blood stream, was not taken up by LSECs even in normal mice which express ApoE. Taken together, a slightly cationic property appears to be essential for recognition by LSECs, and ApoE proteins are not essential but play a subordinate role in delivering siRNA to LSECs, which is quite different from hepatocytes. The YSK15-C4-MEND (pK_a 7.10) showed the strongest gene-silencing activity in LSECs but no gene silencing in other organs was found (**Supplementary Figure S3**), suggesting that the slightly cationic MEND is recognized by some LSEC-specific characteristics including a scavenger function but not by the common characteristics of endothelial cells.[29]

Formulations for delivering siRNA delivery to LSECs have already been reported. Khan *et al.* reported on the development of ionizable amphiphilic dendrimer-based nanomaterials and showed significant gene silencing in LSECs at 0.5 mg/kg.[30] They showed that the use of a larger sized formulation resulted in increased LSEC specificity. However, the amount of cholesterol used between smaller and larger formulations was different. Therefore, the issue of whether the LSEC specificity resulted from a difference of the size or the composition remains unclear. Additionally, gene-silencing activity in other organs was not reported. Dahlman *et al.* reported on the development of polymeric nanoparticles and reported highly efficient gene silencing in endothelial cells in many organs (*e.g.*, lung, heart, and kidneys).[31] The findings reported herein indicate that several factors, including the apparent pK_a value, lipase sensitivity, and particle size, are important to determine the specificity of siRNA delivery to hepatocytes and LSECs. The YSK15-C4-MEND showed an ED_{50} value of 0.1 mg/kg in LSECs, which is the most efficacious in LSECs reported to date, and no gene-silencing activity in other organs. This specific and efficient siRNA formulation provides us with a way to investigate the functions of the LSECs *in vivo*.

The gene-silencing activity of the YSK13-C3-MEND in LSECs was enhanced by a cotreatment with GSK264220A (**Figure 4b**), indicating that the YSK13-C3-MEND is inactivated by the activity of EL. Additionally, as shown in **Supplementary Figure S4**, no significant change in the gene-silencing efficiency of the YSK13-C3-MEND was observed as the result of the GSK264220A cotreatment. This result is supported by the fact that EL is present on the surface of endothelial cells but not hepatocytes in mice.[22] Taken together with the facts that the EL is primarily an A1 phospholipase (PLA1) and that the GSK264220A inhibits the PLA1 activity of the EL,[21] it can be estimated that the YSK13 is cleaved by the PLA1 activity of the EL. Additionally, PLA1 activity of the HL, which is present on the surface of hepatocytes, is known to be much lower than that of EL.[21,32] There are two possible explanations for the result of an above experiment. First, even if the YSK13 were a substrate of the HL, the contribution of the HL would be negligible because the PLA1 activity of the HL is very low. Second, the YSK13 cannot be a substrate of the HL. In any event, these findings suggest that the PLA1 activity of the EL dominantly contributes to decreasing the gene-silencing activity of the YSK13-C3-MEND on the surface of LSECs. Further investigations as to whether other PLA activities degrade an ester bond of the YSK13 are needed. However, to our knowledge, this is the first report of a mechanism that explains such a high level of hepatocyte-specific gene silencing. Since all of the YSK13-MENDs and YSK15-MENDs were on the same sigmoid curve in a plot of pK_a value versus CD31 expression (**Figure 3b**), other YSK13 analogues and YSK15 would be expected to be inactivated by EL as well as YSK13-C3, which indicates that the direction of the ester bond does not affect degradability by EL. Based on these findings, work is now underway to develop a lipase-resistant pH-sensitive cationic lipid and more efficient siRNA delivery formulation in LSECs. The lipase-resistant formulation will enable us to analyze the function of LSECs in lipid metabolism, immune response, and tumor metastasis *in vivo*.

As shown in **Figure 5b**, efficient gene silencing in LSECs was observed for particles with sizes up to 200 nm, which is larger than the size of the fenestrae (average of 120 nm in mice).[33] This result indicates that the MEND was taken up by LSECs from the luminal side and did not need to pass through the fenestrae. It is known that LSECs contain numerous clathrin-coated pits and aggressively pinocytose colloidal particles with sizes less than 200 nm,[29] which corresponds to the finding of a significant reduction of gene-silencing efficiency on LSECs in the case of 420 nm. In hepatocytes, gene-silencing efficiency of the 117- and 172-nm-sized YSK13-C3-MENDs was ~90 and 70% at a dose of 0.1 mg/kg. Based on the dose–response curve of the FVII gene silencing of the YSK13-C3-MEND (data not shown), this 20% difference corresponds to approximately a threefold difference in the dose of siRNA. Taken together with this fact, the ED_{50} value of the YSK15-C4-MEND in hepatocytes (0.4 mg/kg in 79 nm size) can be estimated to be above 1 mg/kg, which is more than 10-fold higher than the ED_{50} value in LSECs (0.1 mg/kg). Therefore, adjusting particle size to ~200 nm is an important factor in increasing LSEC specificity.

In summary, we report on the preparation of a series of LNPs with different physicochemical properties including pK_a value, lipase sensitivity and particle size, which are important factors for cell-specific siRNA delivery. Both the hepatocyte-specific and efficient LNPs and the most efficacious LSEC-targeted LNPs to date were developed based on these findings. Our current understanding of the relationship between physicochemical properties of LNPs and quality of siRNA delivery will facilitate the development of more sophisticated siRNA delivery system with high efficiency, cell selectivity, and safety.

MATERIALS AND METHODS

Materials. Cholesterol (chol) was purchased from SIGMA Aldrich (St. Louis, MO). PEG-DMG, POPC, and DSPS were purchased from the NOF Corporation (Tokyo, Japan). Ribogreen was purchased from Molecular Probes (Eugene, OR). TRIZOL reagent was purchased from Invitrogen (Carlsbad, CA). TNS was purchased from Wako Chemicals (Osaka, Japan). Recombinant human ApoE3 was purchased from BioVision (Milpitas Boulevard, Milpitas, CA). FITC-conjugated Isolectin B4 was purchased from Vector Laboratories (Burlingame, CA). GSK264220A and orlistat

were purchased from Cayman Chemical (Ann Arbor, MI). The sequences for the sense and antisense strands of siRNAs used in this study are listed in **Supplementary Table S2**. All siRNAs were obtained from Hokkaido System Science (Sapporo, Japan). The sequences for forward and reverse primers used in this study are listed in **Supplementary Table S3**. All primers were obtained from SIGMA Genosys Japan (Ishikari, Japan).

Animals. ICR mice and BALB/c.KOR/Stm Slc-*Apoe*^{shl} mice (used as ApoE-deficient mice) were purchased from Japan SLC (Shizuoka, Japan). All animal experimental protocols were reviewed and approved by the Hokkaido University Animal Care Committee in accordance with the guidelines for the care and use of laboratory animals.

^{31}P NMR spectroscopy. A pH-sensitive cationic lipid, POPC, and DSPS at a molar ratio of 1:1:1 (24 μmol of total lipid) were dissolved in 400 μl chloroform and the solvent were removed on a rotovap to form lipid films. The lipid films were hydrated with 500 μl of 10 mmol/l citrate buffer (pH 4.0) at 60 °C. The lipid dispersion was transferred to NMR tubes. Proton-decoupled ^{31}P NMR spectra were obtained using ECX 400P (JEOL) or ECA 500 (JEOL) spectrometer. Acquisition parameters included 60° pulses, a spectral width of 280 kHz (for ECX 400P) or 350 kHz (for ECA 500) with 32,768 data points, and a 1-second interpulse delay time. The temperature was regulated from 21 to 30 °C. An exponential multiplication corresponding to 50 Hz line broadening was applied to the free induction decays before Fourier transformation. The chemical shift was referenced to external 85% phosphoric acid (H_3PO_4).

Preparation and characterization of MENDs. MENDs were prepared by the tertiary butanol (*t*-BuOH) injection method as previously reported.[9] Briefly, 2,100 nmol of the pH-sensitive cationic lipid, 900 nmol of chol, and 90 nmol of PEG-DMG (corresponding to 3 mol% of total lipid) were dissolved in 400 μl of 90% (vol/vol) aqueous *t*-BuOH. Two hundred microliters of 80 μg siRNA solution was gradually added to the lipid solution with vigorous mixing. The resulting siRNA-lipid solution was then gradually added to 2 ml of 20 mmol/l citrate buffer (pH 4.0) under vigorous mixing. Finally, the *t*-BuOH was removed by ultrafiltration, the solution replaced with phosphate-buffered saline at pH 7.4, and the MENDs were then concentrated.

Large MENDs were prepared by a procedure similar to that used to prepare regular MENDs with the exception that a smaller amount of PEG-DMG was added to the mixed lipid solution and a larger volume of 90% *t*-BuOH was added to give a total volume of 400 μl. As the amount of PEG-DMG decreased from 3.0 to 0.3 mol%, the diameter of the MENDs increased from 75 to ~400 nm.

The size and ζ-potential of the MENDs were measured by a Zetasizer Nano ZS ZEN3600 instrument (Malvern Instruments, Worcestershire, UK). The encapsulation efficiency and recovery ratio of siRNA were measured by RiboGreen assay as previously described.[9] The apparent pK_a of the MENDs was measured by means of a TNS assay as previously described.[9] The apparent pK_a was determined as the pH giving rise to half-maximal fluorescent intensity. The percentage of cationically charged pH-sensitive cationic lipid was calculated using the Henderson–Hasselbalch equation.

Evaluation of biodistribution. ICR mice were injected with the MEND formulating Cy5-siGL3 at a siRNA dose of 0.5 mg/kg. Thirty minutes after administration, tissues were collected, weighted, and homogenized using a Precellys 24 (Birthin Technologies, France) in 1% sodium dodecyl sulfate solution. The resulting homogenates were transferred to black 96-well plates and fluorescence was measured using a Varioscan Flash (Thermo Scientific) with λ_{ex} = 648 nm, λ_{em} = 669 nm.

Observation of intrahepatic siRNA distribution. ICR mice were injected with Cy5-siGL3 formulated in MENDs at a dose of 0.5 or 1 mg/kg. Twenty-five minutes after administration, the mice were injected with FITC-conjugated Isolectin B4 (40 μg/mouse) and liver tissues were collected 30 minutes after MEND treatment. Intrahepatic distribution of siRNA was observed using a Nikon A1 (Nikon, Tokyo, Japan). Images were captured by ×60 objective.

Measurement of plasma coagulation FVII activity. Mice were anesthetized after 24–48 hours after siRNA treatment, and blood was obtained by cardiac puncture and processed to plasma using heparin. Plasma FVII activity was measured using a Biophen FVII chromogenic assay kit (Aniara Corporation) according to the manufacturer's protocol.

Quantification of mRNA expression. Mice were anesthetized at 24 hours after siRNA treatment, and tissues were collected. Approximately 30 mg of tissue was homogenized using a Precellys 24 in 500 μl of TRIZOL reagent. Total RNA was extracted according to manufacturer's protocol. The total RNA (1 μg) was reverse transcribed using a High Capacity RNA-to-cDNA kit (ABI) according to manufacturer's protocol. A quantitative PCR analysis was performed on 2 ng cDNA using a Fast SYBR Green Master Mix (ABI) and Lightcycler 480 system II (Roche). All reactions were performed at a volume of 15 μl.

Toxicological test. ICR mice were injected with siPLK1 formulated in the YSK13-C3-MEND at the indicated doses. Twenty-four hours after treatment, the mice were anesthetized and weighed, and blood was obtained by cardiac puncture and processed to serum. Alanine aminotransferase and aspartate aminotransferase activities in serum were measured using a commercially available kit (Wako Chemicals).

Statistical analysis. Results are expressed as mean ± SD. Statistical comparisons between two groups were evaluated by Student's *t*-test and corrected by analysis of variance for multiple comparisons.

SUPPLEMENTARY MATERIAL

Figure S1. Intrahepatic localization of siRNAs formulated in 3 kinds of YSK15-MENDs (pKa 6.65 - 7.25).
Figure S2. ApoE-dependency of gene silencing in hepatocytes and LSECs.
Figure S3. Efficient and liver specific CD31 gene silencing of YSK15-C4-MEND.
Figure S4. Effect of GSK264220A on FVII gene-silencing activity in liver.
Table S1. Physiological parameters of MENDs.
Table S2. List of siRNA sequences used in this study.
Table S3. List of PCR primers used in this study.
Materials and Methods

ACKNOWLEDGMENTS

This work was supported in parts by grants from the Special Education and Research Expenses of the Ministry of Education, Culture, Sports, Science and Technology (MEXT) of Japan and a Grants-in-Aid for Research Activity Start-up from the Japan Society for Promotion of Science (JSPS). The authors also wish to thank Milton S. Feather for his helpful advice in writing the English manuscript. The authors declare no conflict of interest.

REFERENCES

1. Fire, A, Xu, S, Montgomery, MK, Kostas, SA, Driver, SE and Mello, CC (1998). Potent and specific genetic interference by double-stranded RNA in *Caenorhabditis elegans*. *Nature* **391**: 806–811.
2. Yin, H, Kanasty, RL, Eltoukhy, AA, Vegas, AJ, Dorkin, JR and Anderson, DG (2014). Non-viral vectors for gene-based therapy. *Nat Rev Genet* **15**: 541–555.
3. Adami, RC, Seth, S, Harvie, P, Johns, R, Fam, R, Fosnaugh, K *et al.* (2011). An amino acid-based amphoteric liposomal delivery system for systemic administration of siRNA. *Mol Ther* **19**: 1141–1151.
4. Akinc, A, Zumbuehl, A, Goldberg, M, Leshchiner, ES, Busini, V, Hossain, N *et al.* (2008). A combinatorial library of lipid-like materials for delivery of RNAi therapeutics. *Nat Biotechnol* **26**: 561–569.
5. Tang, L, Yang, J, Liu, W, Tang, X, Chen, J, Zhao, D *et al.* (2009). Liver sinusoidal endothelial cell lectin, LSECtin, negatively regulates hepatic T-cell immune response. *Gastroenterology* **137**: 1498–508.e1.
6. Li, R, Oteiza, A, Sørensen, KK, McCourt, P, Olsen, R, Smedsrød, B *et al.* (2011). Role of liver sinusoidal endothelial cells and stabilins in elimination of oxidized low-density lipoproteins. *Am J Physiol Gastrointest Liver Physiol* **300**: G71–G81.

7. Arteta, B, Lasuen, N, Lopategi, A, Sveinbjörnsson, B, Smedsrød, B and Vidal-Vanaclocha, F (2010). Colon carcinoma cell interaction with liver sinusoidal endothelium inhibits organ-specific antitumor immunity through interleukin-1-induced mannose receptor in mice. *Hepatology* **51**: 2172–2182.
8. Kajimoto, K, Sato, Y, Nakamura, T, Yamada, Y and Harashima, H (2014). Multifunctional envelope-type nano device for controlled intracellular trafficking and selective targeting *in vivo*. *J Control Release* **190**: 593–606.
9. Sato, Y, Hatakeyama, H, Sakurai, Y, Hyodo, M, Akita, H and Harashima, H (2012). A pH-sensitive cationic lipid facilitates the delivery of liposomal siRNA and gene silencing activity *in vitro* and *in vivo*. *J Control Release* **163**: 267–276.
10. Hatakeyama, H, Murata, M, Sato, Y, Takahashi, M, Minakawa, N, Matsuda, A *et al.* (2014). The systemic administration of an anti-miRNA oligonucleotide encapsulated pH-sensitive liposome results in reduced level of hepatic microRNA-122 in mice. *J Control Release* **173**: 43–50.
11. Sakurai, Y, Hatakeyama, H, Sato, Y, Hyodo, M, Akita, H and Harashima, H (2013). Gene silencing via RNAi and siRNA quantification in tumor tissue using MEND, a liposomal siRNA delivery system. *Mol Ther* **21**: 1195–1203.
12. Tamaru, M, Akita, H, Nakatani, T, Kajimoto, K, Sato, Y, Hatakeyama, H *et al.* (2014). Application of apolipoprotein E-modified liposomal nanoparticles as a carrier for delivering DNA and nucleic acid in the brain. *Int J Nanomedicine* **9**: 4267–4276.
13. Watanabe, T, Hatakeyama, H, Matsuda-Yasui, C, Sato, Y, Sudoh, M, Takagi, A *et al.* (2014). *In vivo* therapeutic potential of Dicer-hunting siRNAs targeting infectious hepatitis C virus. *Sci Rep* **4**: 4750.
14. Yamamoto, Y, Sato, Y, Munakata, T, Kakuni, M, Tateno, C, Sanada, T *et al.* (2015). Novel pH-sensitive multifunctional envelope-type nanodevice for siRNA-based treatments for chronic HBV infection. *J Hepatol* (doi:10.1016/j.hep.2015.10.014).
15. Cullis, PR and de Kruijff, B (1979). Lipid polymorphism and the functional roles of lipids in biological membranes. *Biochim Biophys Acta* **559**: 399–420.
16. Bailey, AL and Cullis, PR (1994). Modulation of membrane fusion by asymmetric transbilayer distributions of amino lipids. *Biochemistry* **33**: 12573–12580.
17. Zhang, J, Fan, H, Levorse, DA and Crocker, LS (2011). Ionization behavior of amino lipids for siRNA delivery: determination of ionization constants, SAR, and the impact of lipid pKa on cationic lipid-biomembrane interactions. *Langmuir* **27**: 1907–1914.
18. Jayaraman, M, Ansell, SM, Mui, BL, Tam, YK, Chen, J, Du, X *et al.* (2012). Maximizing the potency of siRNA lipid nanoparticles for hepatic gene silencing *in vivo*. *Angew Chem Int Ed Engl* **51**: 8529–8533.
19. Akinc, A, Querbes, W, De, S, Qin, J, Frank-Kamenetsky, M, Jayaprakash, KN *et al.* (2010). Targeted delivery of RNAi therapeutics with endogenous and exogenous ligand-based mechanisms. *Mol Ther* **18**: 1357–1364.
20. Yan, X, Kuipers, F, Havekes, LM, Havinga, R, Dontje, B, Poelstra, K *et al.* (2005). The role of apolipoprotein E in the elimination of liposomes from blood by hepatocytes in the mouse. *Biochem Biophys Res Commun* **328**: 57–62.
21. Yasuda, T, Ishida, T and Rader, DJ (2010). Update on the role of endothelial lipase in high-density lipoprotein metabolism, reverse cholesterol transport, and atherosclerosis. *Circ J* **74**: 2263–2270.
22. Yu, KC, David, C, Kadambi, S, Stahl, A, Hirata, K, Ishida, T *et al.* (2004). Endothelial lipase is synthesized by hepatic and aorta endothelial cells and its expression is altered in apoE-deficient mice. *J Lipid Res* **45**: 1614–1623.
23. Fuki, IV, Blanchard, N, Jin, W, Marchadier, DH, Millar, JS, Glick, JM *et al.* (2003). Endogenously produced endothelial lipase enhances binding and cellular processing of plasma lipoproteins via heparan sulfate proteoglycan-mediated pathway. *J Biol Chem* **278**: 34331–34338.
24. Goodman, KB, Bury, MJ, Cheung, M, Cichy-Knight, MA, Dowdell, SE, Dunn, AK *et al.* (2009). Discovery of potent, selective sulfonylfuran urea endothelial lipase inhibitors. *Bioorg Med Chem Lett* **19**: 27–30.
25. Andréo, U, Maillard, P, Kalinina, O, Walic, M, Meurs, E, Martinot, M *et al.* (2007). Lipoprotein lipase mediates hepatitis C virus (HCV) cell entry and inhibits HCV infection. *Cell Microbiol* **9**: 2445–2456.
26. Hafez, IM, Maurer, N and Cullis, PR (2001). On the mechanism whereby cationic lipids promote intracellular delivery of polynucleic acids. *Gene Ther* **8**: 1188–1196.
27. Sadzuka, Y, Hirota, S (1997). Physical properties and tissue distribution of Adriamycin encapsulated in polyethyleneglycol-coated liposomes. *Adv Drug Deliv Rev* **24**: 257–263.
28. Mui, BL, Tam, YK, Jayaraman, M, Ansell, SM, Du, X, Tam, YY *et al.* (2013). Influence of polyethylene glycol lipid desorption rates on pharmacokinetics and pharmacodynamics of siRNA lipid nanoparticles. *Mol Ther Nucleic Acids* **2**: e139.
29. Sørensen, KK, McCourt, P, Berg, T, Crossley, C, Le Couteur, D, Wake, K *et al.* (2012). The scavenger endothelial cell: a new player in homeostasis and immunity. *Am J Physiol Regul Integr Comp Physiol* **303**: R1217–R1230.
30. Khan, OF, Zaia, EW, Yin, H, Bogorad, RL, Pelet, JM, Webber, MJ *et al.* (2014). Ionizable amphiphilic dendrimer-based nanomaterials with alkyl-chain-substituted amines for tunable siRNA delivery to the liver endothelium *in vivo*. *Angew Chem Int Ed Engl* **53**: 14397–14401.
31. Dahlman, JE, Barnes, C, Khan, OF, Thiriot, A, Jhunjunwala, S, Shaw, TE *et al.* (2014). *In vivo* endothelial siRNA delivery using polymeric nanoparticles with low molecular weight. *Nat Nanotechnol* **9**: 648–655.
32. Duong, M, Psaltis, M, Rader, DJ, Marchadier, D, Barter, PJ and Rye, KA (2003). Evidence that hepatic lipase and endothelial lipase have different substrate specificities for high-density lipoprotein phospholipids. *Biochemistry* **42**: 13778–13785.
33. Snoeys, J, Lievens, J, Wisse, E, Jacobs, F, Duimel, H, Collen, D *et al.* (2007). Species differences in transgene DNA uptake in hepatocytes after adenoviral transfer correlate with the size of endothelial fenestrae. *Gene Ther* **14**: 604–612.